World-to-chip microfluidic interface with built-in valves for multichamber chip-based PCR assays

Kwang W. Oh,* Chinsung Park, Kak Namkoong, Jintae Kim, Kyeong-Sik Ock, Suhyeon Kim, Young-A Kim, Yoon-Kyoung Cho and Christopher Ko

Received 8th March 2005, Accepted 16th May 2005 First published as an Advance Article on the web 23rd June 2005 DOI: 10.1039/b503437j

We report a practical world-to-chip microfluidic interfacing method with built-in valves suitable for microscale multichamber chip-based assays. One of the primary challenges associated with the successful commercialization of fully integrated microfluidic systems has been the lack of reliable world-to-chip microfluidic interconnections. After sample loading and sealing, leakage tests were conducted at 100 °C for 30 min and no detectable leakage flows were found during the test for 100 microchambers. To demonstrate the utility of our world-to-chip microfluidic interface, we designed a microscale PCR chip with four chambers and performed PCR assays. The PCR results yielded a 100% success rate with no contamination or leakage failures. In conclusion, we have introduced a simple and inexpensive microfluidic interfacing system for both sample loading and sealing with no dead volume, no leakage flow and biochemical compatibility.

1. Introduction

Over the last decade microfluidic research has intensively focused on the development of fully integrated microfluidic on-chip biochemical systems, lab-on-a-chip (LOC) or micro total analysis systems (μ -TAS). ¹⁻¹¹ The biochemical systems, including polymerase chain reaction (PCR), ¹¹⁻¹⁷ DNA analysis and sequencing, ^{18,19} protein separation, ^{20,21} immunoassay, ^{22–26} and cellular analysis, ^{27–30} have been reduced in size to a micro scale chip. Major advantages of this miniaturization are the drastic decrease in chemical reaction time and reduction in expensive chemical reagents.

From a practical solution standpoint, one of the stumbling blocks associated with the successful miniaturization and commercialization of fully integrated microfluidic systems has been the development of reliable world-to-chip interfaces, which allow easy coupling between the macro scale in the real world and the micro scale in the microfluidic devices. 31-40 Most monolithic microfluidic devices (e.g. micro PCR chips, microfluidic-based reactors and sensors) have several inlets, outlets, or vents which are coupled to the macro environment using pipettes, tubes and Luer fittings. To date, the most common approach to loading samples or reagents to the monolithic microfluidic devices has been the use of epoxy based adhesives. However, the use of adhesives at world-tochip interconnects has often been known to generate problems with leakage flow, dead volume, temperature stability, contamination and biochemical compatibility. 40-42

In addition to sample loading function, sealing or valving of the inlet, outlet or vent ports is a critical feature in ensuring successful biochemical assays such as polymerase chain reaction. It is known that evaporation of reagents and air bubble generation cause PCR reactions to fail. Therefore, it is

Bio Lab, Samsung Advanced Institute of Technology, P.O. Box 111, Suwon, 440-600, Korea. E-mail: MrOhio@Samsung.com imperative that the valves should tightly seal the ports when loading samples but be easily re-opened to allow the post-PCR products to flow into downstream for further detection and analysis.

The importance of world-to-chip microfluidic interface has been heightened as the need to have multiple chambers on a single chip has emerged from the molecular diagnostic field. For qualitative clinical diagnostics, it is likely that the chip would require at least three chambers: a test sample, a negative control, and a positive control. Also, for quantitative applications, multiple chamber format is useful in holding an unknown sample with a set of known standard samples. Therefore, it is essential that for molecular diagnostics, multiple assays need to be carried out on a single chip.

To deal with the above issues, we have proposed a multiple microfluidic interfacing system with built-in valves which provides no dead volume, no leakage flow, and biochemical compatibility. Our system is simple and inexpensive to fabricate, and is easy to interface with the real world by using conventional pipette tips. The feasibility of our world-to-chip microfluidic interfacing system has been proven by performing for the first time, as far as we are aware, multichamber chipbased PCR reactions.

2. Microfluidic interface

2.1 Concept

Fig. 1 shows schematic views of the dual mode microfluidic interfacing technology suitable for sample loading and sealing. Plastic fittings, which contain pipette tip guides and a rubber sheet, were set to accommodate conventional pipette tips for sample loading by aligning tips to the inlet holes (Fig. 1(a)). Without the pipette tip guides, it would be difficult to align the pipette tips to each hole and load samples efficiently. Once samples are loaded to microchambers, the plastic fittings with

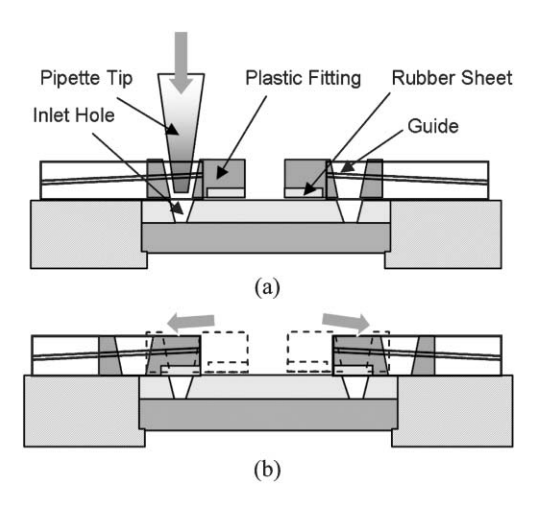


Fig. 1 Schematic views of the dual mode microfluidic interfacing technology for both sample loading and sealing. (a) Sample loading mode: plastic fittings, which contain the pipette tip guides and the rubber sheet, are set to accommodate conventional pipette tips for sample loading by aligning tips to the inlet holes. (b) Sample sealing mode: once samples are loaded to microchambers, the plastic fittings with the rubber sheet can be slid to the position of the sealing mode to enclose the inlets/vents without dead volume.

the rubber sheet can be slid to the position of the sealing mode to enclose the inlets/vents without dead volume (Fig. 1(b)). In order to resist the internal pressure build-up during thermal cycling, flexible PDMS rubber sheets are used as sealing materials; in the guiding mode the sheets are not pressurized to assist an easy sliding of the fittings, but in the sealing mode the sheets are designed to be pressurized.

2.2 Design and manufacturing

Multichamber micro PCR chip. Fig. 2 shows mask layouts of a multichamber micro PCR chip and a silicon-based heater plate with a built-in temperature sensor. For successful optical detection and thermal reaction, the design and fabrication of

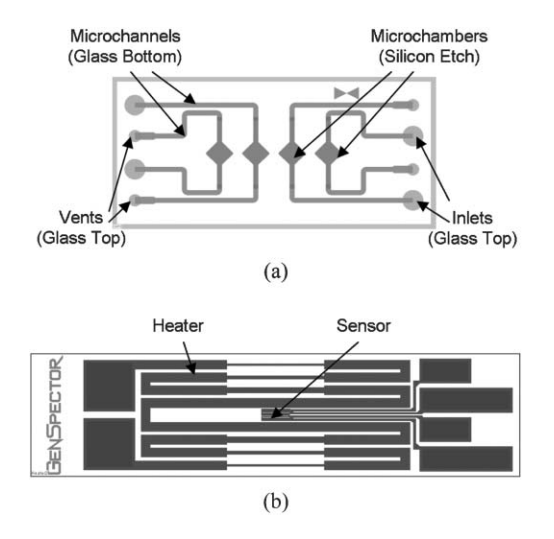


Fig. 2 Mask layouts of (a) the multichamber micro PCR chip (13 mm \times 6 mm \times 1 mm) and (b) the external silicon plate (20 mm \times 5 mm \times 0.5 mm) with a heater and a sensor.

each chamber should be carefully carried out considering the chamber volume and temperature uniformity. Since *in-situ* monitoring is being performed optically through the glass windows covering the chambers, we designed the length and volume of microchannels to be identical. To minimize the microchannel volume the size of vent holes (200 μ m in diameter) was designed to be much less than that of inlet holes (800 μ m in diameter).

In addition to the identical physical dimension in each microchannel and microchamber, an uniform temperature distribution during the thermal reaction is desirable. The temperature uniformity in the multichamber PCR chip has been verified by simulation using the CFD-ACE tool (CFD Research Corporation, Huntsville, AL). Fig. 3(a) shows the simulation result of average temperature differences between the first two microchambers from the left end or from the right end with the thermal cycling profile. Maximum temperature difference occurred at t = 3 s when the initial ramping from 63 °C to 93 °C with a ramping rate of 10 °C s⁻¹ ends. Fig. 3(b) shows 3-dimensional temperature contours in the microchambers and microchannels at 3 s, 4 s, 10 s, and 24 s, and the corresponding times are marked with dotted lines in Fig. 3(a). Overall temperature differences were within 0.01 °C, which are good enough for uniform PCR yields.

The fabrication processes for the micro PCR chip consisted of four photolithography steps: silicon etch, glass top, glass bottom, and heater/sensor. 12 The silicon wafer with a thickness of 500 µm was etched to a depth of 280 µm by silicon wet etching solution (25% TMAH) to form the microchambers with a volume of 0.95 μL. A 3500 Å silicon dioxide layer was grown on the surface of reaction chamber for the purposes of passivation. 11-14 The wet etched silicon wafer was anodically bonded with the glass substrate with inlet/vent holes and microchannels formed by a sand blast technique. The inlet holes formed on the top side of the glass substrate were designed to fit into the shape of the pipette tips. The microchannels with a width of 100 µm and a depth of 100 μm were formed on the bottom side of the glass substrate. The external silicon-based heater/sensor plate, formed by evaporating a thin film layer of Ti/Pt, was physically separated from the micro PCR chip and can be used permanently after initial temperature calibration.

Cartridge. As shown in Fig. 4(a), a cartridge consisted of a 4-chamber micro PCR chip (Fig. 4(b)), two plastic fittings and a plastic chip holder. The cartridges as shown in Fig. 4(c) were easily assembled as following: First, the micro PCR chip with a dimension of 13 mm \times 6 mm \times 1 mm was inserted to the holder. Second, the plastic fittings with the rubber sheet were assembled with the holder, as shown in the dotted lines in Fig. 4(a).

PDMS material as the rubber sheet was selected for biochemical compatibility and the fittings were designed to withstand at least 8.1 Psi. ¹⁴ If sealing or valving using the rubber sheet fails, the PCR sample will be pushed out of the microchamber, resulting in a failed PCR. The amount of pressure required to prevent degassing was estimated to be ~ 3.1 Psi. ⁴³ In the worst case, the presence of air bubbles between the rubber sheet and the inlets/vents will cause an

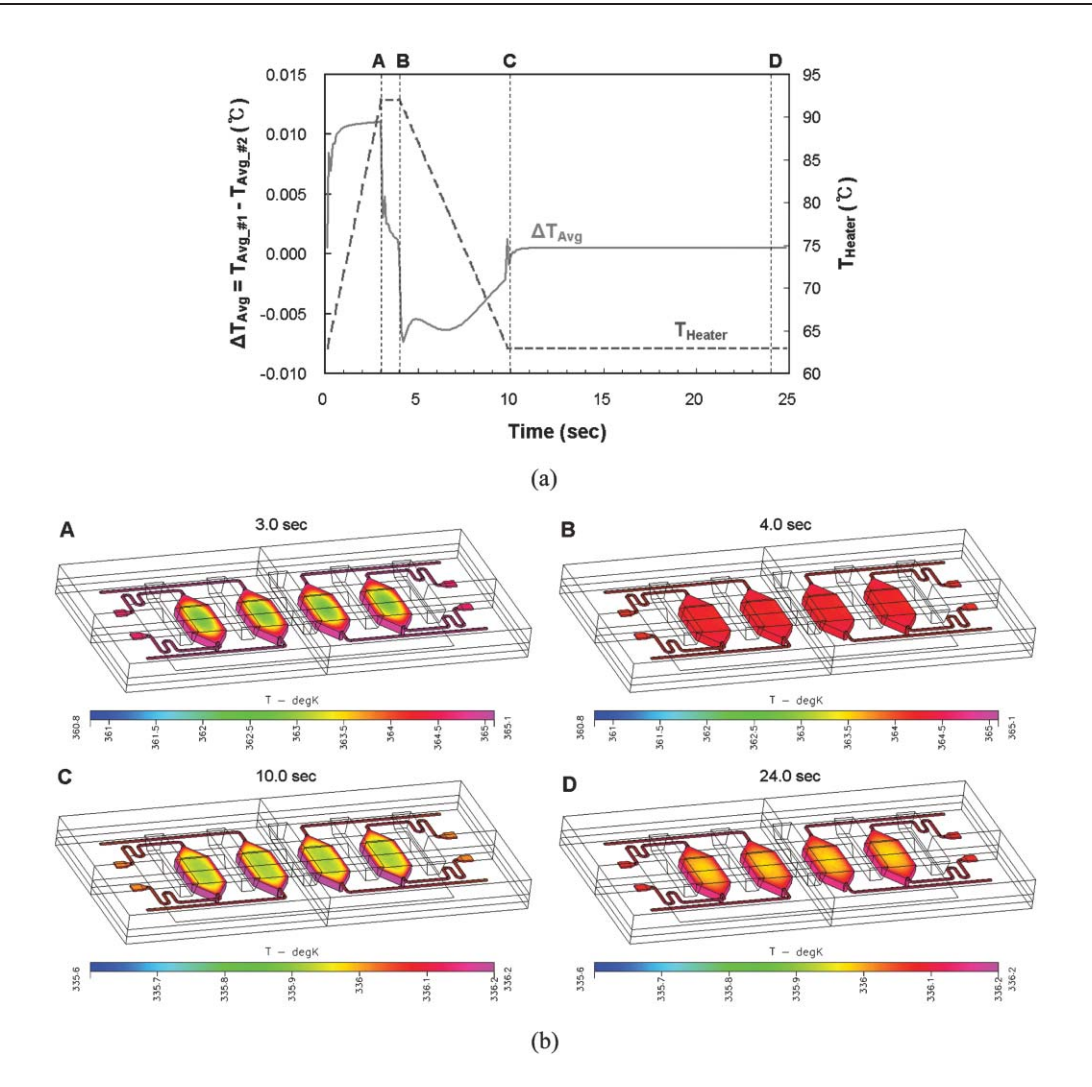


Fig. 3 (a) The CFD-ACE simulation result of average temperature differences (—) between two neighbor microchambers with the thermal cycling profile (---). Maximum temperature difference occurred at t = 3 s when the initial ramping from 63 °C to 93 °C with a ramping rate of 10 °C s⁻¹ ends. (b) The 3-dimensional temperature contours in the micro PCR chip at 3 s (A), 4 s (B), 10 s (C), and 24 s (D). Overall temperature differences were within 0.01 °C, which are good enough for uniform PCR yields.

additional internal pressure build-up of 3.7 Psi at 94 °C;⁴⁴ therefore, the rubber sheet has to withhold at least the internal pressure of 6.8 psi. The pressure P on the rubber surface is

$$P = E \frac{\delta L}{L},\tag{1}$$

where E is Young's modulus of elasticity, L is a total length of the rubber, and δL is an elongation length. The elongation length between two modes for sample loading and sealing was designed to be 0.15 mm, where the original length of the rubber sheet was 2 mm. By using (1), the enclosure pressure of 8.1 Psi was calculated, when the Young's modulus of the PDMS was assumed to be 750 kPa.

Module. The plastic cartridge packaged with the 4-microchamber silicon micromachined PCR chip can be inserted in each micro PCR module as shown in Fig. 4(d). The module had the external silicon-based heater plate with a built-in temperature sensor, a cooling fan, an optic unit for both excitation and detection of fluorescent dyes, and a computing

board with an embedded microprocessor. Consequently, each module was capable of independent thermal cycling and in-situ monitoring of the micro PCR chips. Independent PID (proportional integral derivative) control by the embedded microprocessor in each module can give an excellent temperature accuracy of less than 0.5 °C for PCR.

2.3 Results and discussion

Once the cartridges were assembled with the PCR chip, they were ready for sample loading and sealing. The world-to-chip microfluidic interconnection technology with dual functions of sample loading and sealing for the multichamber micro PCR chip has been successfully demonstrated as shown in Fig. 5. For easy viewing, the sample was mixed with a red-color dye and only three microchambers were filled.

A pipette tip (Eppendorf, 10 μL S) holding a 1 μL sample was easily inserted into microchamber #1 by the help of the pipette tip guide #1 (Fig. 5(a): pipette guide mode). Due to the

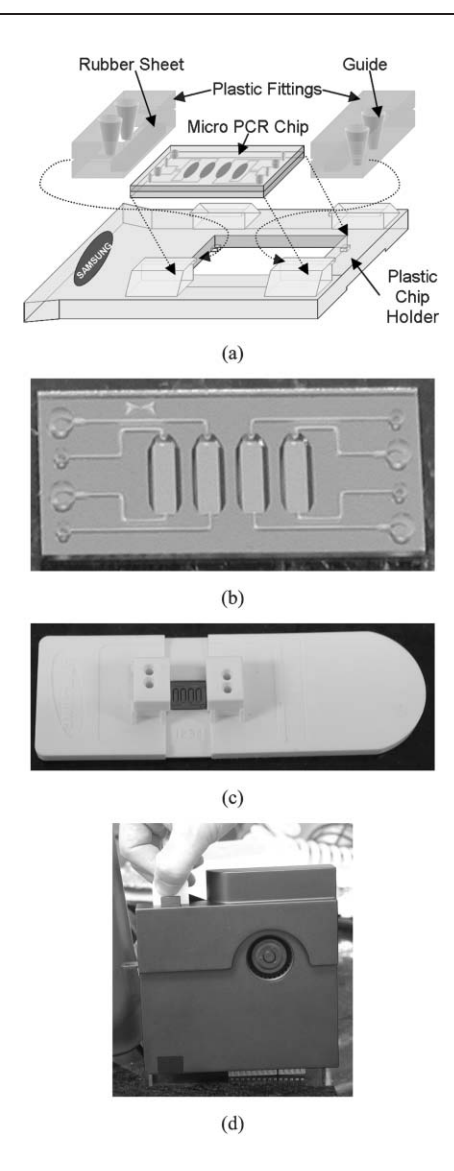


Fig. 4 (a) Schematic view of the assembly process. Photographs of (b) the 4-microchamber micro PCR chip with dimesions of 13 mm \times 6 mm \times 1 mm, (c) the assembled cartridge with the PCR chip, and (d) the module for the real-time PCR with the inserted cartridge.

SiO₂ surface coating of the microchannels and the microchambers, the fluid can be loaded by a capillary force. To minimize bubble formation, dead volume also should be minimized in the microfluidic devices. In this demonstration, no bubbles inside the microchambers were generated during sample loading into inlet #1, #2, and #3 (Fig. 5(b)–(d): sample loading). Once the samples are loaded, the pipette guide and sample loading mode are switched to the sealing mode by sliding the plastic fittings. To ensure the exact positioning of the fittings, a simple device was used (Fig. 5(e): sliding of the plastic fittings to enclose the inlets/vents): The device was capable of guiding the pipette tips, in addition to sliding the fittings from the loading mode to the sealing mode. Three microchambers #1, #2, and #3 were successfully filled with the fluids and microchamber #4 was a blank without the fluid (Fig. 5(f): sample sealing mode).

The leakage test was conducted by elevating the temperature to $100~^{\circ}\text{C}$ for 30 min in a convection oven, after sample loading

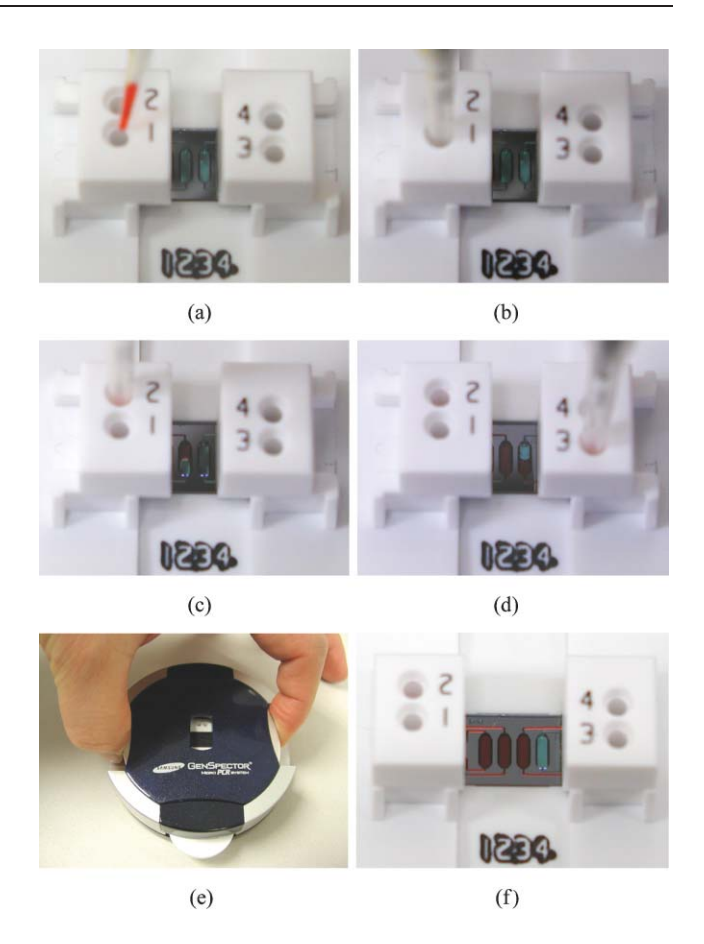


Fig. 5 Demonstration for the practical world-to-chip microfluidic interfacing technology (only microchamber #1, #2, #3 are loaded for comparison, as shown in (f)): (a) pipette guide mode, (b) sample loading (inlet #1), (c) sample loading (inlet #2), (d) sample loading (inlet #3), (e) plastic fittings are sliding to enclose the inlets/vents using the small device capable of sliding the fittings from the loading mode to the sealing mode, and (f) sample sealing mode.

and sealing. No detectable leakage flows have been found during the test, except for two microchambers from 25 cartridges (n=100 microchambers). A sealing success rate of 98% was achieved.

3. Real-life application

3.1 Micro PCR

The polymerase chain reaction is a well-known DNA amplification method useful for genetic identification and gene diagnostics. $^{11-17}$ Typically the method requires a repeated three thermal steps: denaturation at 95 °C, annealing at 55 °C and extension at 72 °C. $^{11-14}$ Compared to the conventional PCR method, which requires more than two hours, microscale based PCR chips, due to silicon's high thermal conductivity and reduced sample volume (1 μL), can finish the amplification in less than 25 min.

In addition to the function of sample loading into the microfluidic devices, sealing of the inlet, outlet or vent ports is a critical function to successfully carrying out PCR. The valves have to resist the internal pressure generated all through thermal cycling up to $100~^{\circ}\text{C}$ and should be re-opened easily

after PCR. The valve materials should be compatible to PCR, because valves will be in direct contact with the PCR reagent. To demonstrate the utility of the suggested world-to-chip microfluidic interfacing technology a multichamber micro PCR chip has been designed and tested.

3.2 PCR experiment

Each microchamber in the micro PCR chip was first loaded and sealed as previously described, with a total volume of 1 µL reaction reagent, containing 1 × SYBR® Green I PCR buffer (PE Biosystems), 1 mM of forward and reverse primers (Genotech, Korea), each 200 µM dNTP (deoxynucleoside triphosphates) (Sigma), 5 mM MgCl₂ (Sigma), 5% glycerol (Sigma), 500 mM formamide (Promega), 0.2 ng μL⁻¹ BSA (Sigma), 0.01 unit μL^{-1} Uracil-N-glycosylase (Sigma), and 0.1 unit μL^{-1} Taq polymerase (Solgent. Co, Ltd, Korea). For these reactions a HBV plasmid DNA was used as a PCR template. 50 cycles of denaturation at 92 °C for 1 s and annealing-extension step at 62 °C for 15 s were performed. During the thermal cycling, relative fluorescence intensity was monitored in real-time (Fig. 6(a)). After amplification cycles were completed, a melting curve was obtained by heating the chip from 60 to 90 °C (Fig. 6(c)). The total time required for the 50 cycles of amplification and the melting analysis was less than 25 min.

3.3 Results and discussion

For the real-life application of the world-to-chip microfluidic interface with built-in valves, multiple PCR assays with different initial copies of HBV plasmid DNA have been conducted: 10^5 , 10^6 , 10^7 , and 10^8 copies μL^{-1} were loaded and sealed in each microchamber #1, #2, #3, and #4, respectively. For the real-time monitoring, SYBR® Green I, an intercalating dye with a specificity for the double stranded DNA, was used in the PCR assays. The results are shown in Fig. 6(a). The cycle number at which PCR efficiency is maximized is defined as $C_{\rm T}$ in this work. ^{45–47} A set of $C_{\rm T}$ values can be converted as a function of the known initial copy numbers, so called a standard curve of quantitative PCR, as shown in Fig. 6(b). After the real-time PCR was completed, a melting curve was obtained by slowly heating with a ramping rate of 0.1 °C s⁻¹ as shown in Fig. 6(c). The melting temperature $(T_{\rm m})$ has been widely used to identify the amplified PCR products, since the melting temperature can be used for the identification of the specific target products. The average $T_{\rm m}$ from 4 independent assays was 77.73 \pm 0.11 °C with the coefficient of variation (CV) of 0.15%.

Results of four assays with the single chip were summarized in Table 1. To validate the on-chip assay results, an off-chip analysis was performed; the PCR products were removed from the chip and analyzed by a LabChip device (Caliper

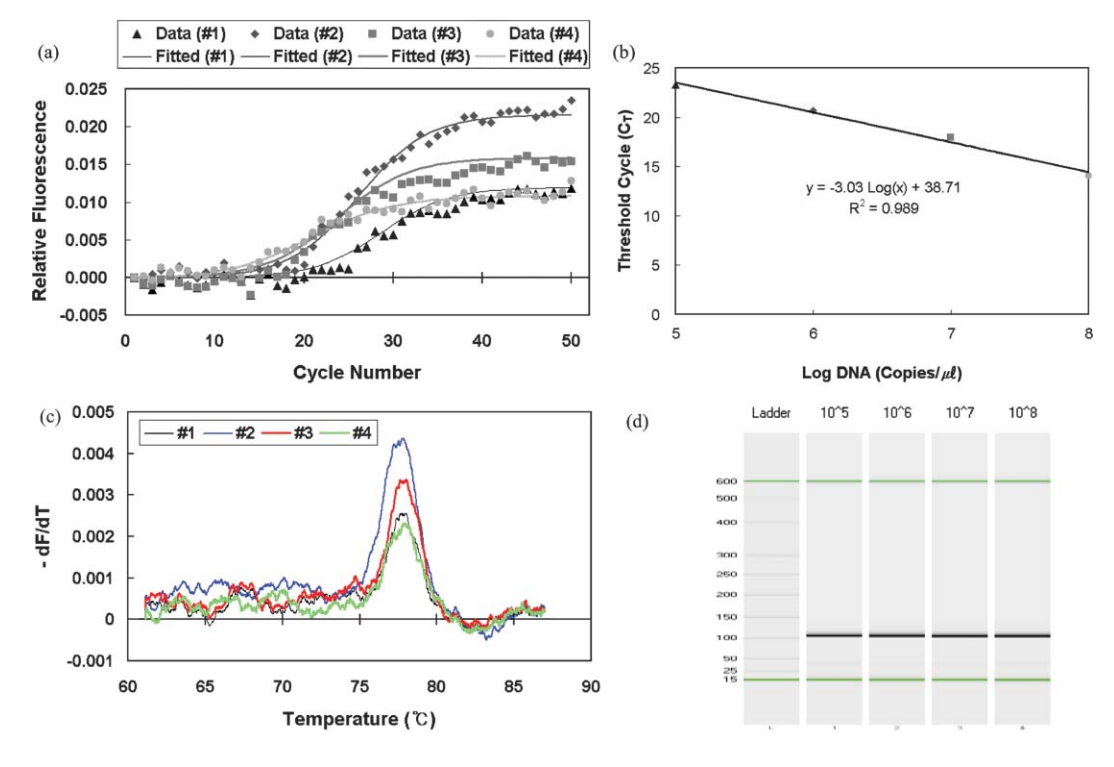


Fig. 6 Results of real-life application of the world-to-chip microfluidic interfaces: On-chip and off-chip analyses of multiple PCR assays in the single micro PCR chip. (a) Real-time PCR is conducted using the HBV plasmid DNA and SYBR[®] Green I with 4 different concentrations of 10^5 copies μL^{-1} (\clubsuit), 10^6 copies μL^{-1} (\spadesuit), 10^7 copies μL^{-1} (\blacksquare), and 10^8 copies μL^{-1} (\blacksquare). The optic unit for detection of fluorescent signals has not been optimized yet in terms of calibration of each silicon photodiode detector in the unit. (b) A set of C_T values are converted as a function of the known initial copy numbers, so called a standard curve of quantitative PCR. An R^2 value of 0.989 was obtained using the slope of the best fitted line. (c) After the sample reaches the plateau phase, melting curves are acquired and converted into melting peaks for the identification of the PCR product. (d) The amplified PCR products are analyzed by a LabChip device (Caliper Lifesciences) and a Bioanalyzer 2100 (Agilent Technologies), by re-opening the inlets/vents and followed by pipetting out the amplified products from each multichamber.

Table 1 Results of real-life application of the world-to-chip microfluidic interface: on-chip (cf. Fig. 6(a), (b), and (c)) and off-chip (cf. Fig. 6(d)) analyses of multiple PCR assays in the single Micro PCR

Microchamber		#1	#2	#3	#4
Off-chip	HBV Sample (copies μL^{-1}) Threshold cycle (C_T) Melting temperature (°C) Base pair (bp) Concentration (ng μL^{-1})	23.27 77.75 106	77.57 105	10 ⁷ 17.98 77.83 105 31.0	14.05

^a On-chip analysis means real-time PCR monitoring of the PCR reagents and melting curve monitoring of the amplified PCR products without taking out the products. b Off-chip analysis means gel-based analysis by taking out the products from the chip.

Lifesciences) and a Bioanalyzer 2100 (Agilent Technologies), as shown in Fig. 6(d). The amplified products matched well with the expected HBV DNA (~ 105 bp). The predicted melting temperature based on G-C contents was 80 °C (Primer Express® software version 2.0 from Applied Biosystems).

4. Conclusion

In conclusion, we have designed and tested a world-to-chip microfluidic interfacing method with built-in valves, which provides no dead volume, no leakage flow, and biochemical compatibility. This interface performed excellently in both loading the samples and sealing the reagents, as evidenced in successfully performing real-time multiple PCR assays. We believe that the multichamber lab-on-chips will become invaluable tools for molecular diagnostics and the success of multichamber chips will depend on the availability of microfluidic interfaces with built-in valves. The world-to-chip interfacing technology can be easily packaged into a next generation hand-held real-time PCR system, which is currently underway.

Notes and references

- 1 C. H. Ahn, J.-W. Choi, G. Beaucage, J. H. Nevin, J.-B. Lee, A. Puntambekar and Y. Lee Jae, Proc. IEEE, 2004, 92, 154-173.
- 2 A. E. Kamholz, Lab Chip, 2004, 4, 16N-20N.
- 3 D. J. Laser and J. G. Santiago, J. Micromech. Microeng., 2004, 14, R35-R64
- 4 A. J. de Mello and N. Beard, Lab Chip, 2003, 3, 11N-19N.
- 5 H. Andersson and A. van den Berg, Sens. Actuators B, 2003, 92, 315-325.
- 6 R. Ehrnström, Lab Chip, 2002, 2, 26N-30N.
- 7 Y. Huang, E. L. Mather, J. L. Bell and M. Madou, Anal. Bioanal. Chem., 2002, 372, 49-65.
- 8 M. Krishnan, V. Namasivayam, R. Lin, R. Pal and M. A. Burns, Curr. Opin. Biotechnol., 2001, 12, 92-98.
- 9 M. Madou and J. Florkey, Chem. Rev., 2000, 100, 2679-2692.
- 10 C. H. Mastangelo, M. A. Burns and D. T. Burke, Proc. IEEE, 1998, **86**, 1769–1787.
- 11 L. J. Kricka and P. Wilding, Anal. Bioanal. Chem., 2003, 377,
- 12 D. S. Yoon, Y.-S. Lee, Y. Lee, H. J. Cho, S. W. Sung, K. W. Oh, J. Cha and G. Lim, J. Micromech. Microeng., 2002, 12, 813-823.
- 13 K. W. Oh, Y.-K. Cho, J. Kim, S. Kim, K.-S. Ock, K. Namkoong, K. Yoo, C. Park, Y. Lee, Y.-A. Kim, J. Han, H. Lim, J. Kim, D. Yoon, G. Lim, S. Kim, J.-J. Hwang and Y. E. Pak, Micro Total Analysis System 2004, Malmo, RSC, Cambridge, 2004, vol. 1, pp. 150-152.

- 14 K. W. Oh, C. Park and K. Namkoong, IEEE 18th International Conference on Micro Electro Mechanical Systems (MEMS 2005), Miami, 2005, pp. 714-717.
- 15 E. T. Lagally, C. A. Emrich and R. A. Mathies, Lab Chip, 2001, 1, 102-107.
- 16 M. A. Burns, B. N. Johnson, S. N. Brahmasandra, K. Handique, J. R. Webster, M. Krishnan, T. S. Sammarco, P. M. Man, D. Jones, D. Heldsinger, C. H. Mastrangelo and D. T. Burke, Science, 1998, **282**, 484-487.
- 17 R. H. Liu, J. Yang, R. Lenigk, J. Bonanno and P. Grodzinski, Anal. Chem., 2004, 76, 1824-1831.
- 18 A. T. Woolley, D. Hadley, P. Landre, A. J. deMello, R. A. Mathies and M. A. Northrup, Anal. Chem., 1996, 23, 4081-4086.
- N. Goedecke, B. McKenna, S. El-Difrawy, L. Carey, P. Matsudaira and D. Ehrlich, *Electrophoresis*, 2004, 25, 1678–1686.
- 20 A. G. Hadd, D. E. Raymond, J. W. Halliwell, S. C. Jacobson and J. M. Ramsey, Anal. Chem., 1997, 69, 3407-3412.
- 21 A. E. Herr, J. I. Molho, K. A. Drouvalakis, J. C. Mikkelsen, P. J. Utz, J. G. Santiago and T. W. Kenny, Anal. Chem., 2003, 75, 1180-1187
- 22 N. Chiem and D. J. Harrison, Anal. Chem., 1997, 69, 373-378.
- 23 K. Sato, M. Yamanaka, H. Takahashi, M. Tokeshi, H. Kimura and T. Kitamori, Electrophoresis, 2002, 23, 734-739.
- 24 J. Moorthy, G. A. Mensing, D. Kim, S. Mohanty, D. T. Eddington, W. H. Tepp, E. A. Johnson and D. J. Beebe, Electrophoresis, 2004, **25**, 1705–1713.
- 25 J.-W. Choi, K. W. Oh, J. H. Thomas, W. R. Heineman, H. B. Halsall, J. H. Nevin, A. J. Helmicki, H. T. Henderson and C. H. Ahn, Lab Chip, 2002, 2, 27–30.
- 26 J.-W. Choi, K. W. Oh, A. Han, C. A. Wijayawardhana, C. Lannes, S. Bhansali, K. T. Schlueter, W. R. Heineman, H. B. Halsall, J. H. Nevin, A. J. Helmicki, H. T. Henderson and C. H. Ahn, Biomed. Microdevices, 2001, 3, 191-200.
- 27 D. T. Chiu, N. L. Jeon, S. Huang, R. S. Kane, C. J. Wargo, I. S. Choi, D. E. Ingber and G. M. Whitesides, Proc. Natl. Acad. Sci. USA, 2000, 97, 2408–2413.
- E. Tamaki, K. Sato, M. Tokeshi, K. Sato, M. Aihara and T. Kitamori, Anal. Chem., 2002, 74, 1560-1564.
- 29 P. C. H. Li and D. J. Harrison, Anal. Chem., 1997, 69, 1564–1568.
- 30 E. A. Schilling, A. E. Kamholz and P. Yager, Anal. Chem., 2002, **74**, 1798–1804.
- 31 C. K. Fredrickson and Z. H. Fan, Lab Chip, 2004, 4, 526-533.
- 32 V. Nittis, R. Fortt, C. H. Legge and A. J. de Mello, Lab Chip, 2001, 1, 148-152
- 33 A. Puntambekar and C. H. Ahn, J. Micromech. Microeng., 2002, **12**, 35–40.
- 34 C. Gonzalez, S. D. Collins and R. L. Smith, Sens. Actuators B, 1998, 49, 40-45.
- 35 H. Chen, D. Acharya, A. Gajraj and J.-C. Melners, Anal. Chem., 2003, 75, 5287-5291.
- 36 J. M. Ramsey, *Nat. Biotechnol.*, 1999, 17, 1061–1062.
 37 S. Attiya, A. B. Jemere, T. Tang, G. Fitzpatrick, K. Seiler, N. Chiem and D. J. Harrison, Electrophoresis, 2001, 22, 318–327.
- 38 N. H. Bings, C. Wang, C. D. Skinner, C. L. Colyer, P. Thibault and D. J. Harrison, Anal. Chem., 1999, 71, 3292-3296.
- 39 J. Liu, C. Hansen and S. R. Quake, Anal. Chem., 2003, 75, 4718-4723.
- 40 Z. Yang and R. Maeda, J. Chromatogr. A, 2003, 1013, 29-33.
- 41 A. V. Pattekar and M. V. Kothare, J. Micromech. Microeng., 2003, **13**, 337–345.
- 42 B. L. Gray, D. Jaeggi, N. J. Mourlas, B. P. van Drieenhuizen, K. R. Williams, N. I. Maluf and G. T. A. Kovacs, Sens. Actuators, 1999, 77, 57-65.
- 43 J. Chiou, P. Matsudaira, A. Sonin and D. Ehrlich, Anal. Chem., 2001, 73, 2018–2021.
- Y. Liu, B. Rauch Cory, L. Stevens Randall, Ralf Lenigk, Jianing Yang, B. Rhine David and Piotr Grodzinski, Anal. Chem., 2002, 74, 3063-3070.
- 45 M. S. Ibrahim, R. S. Lofts, P. B. Jahrling, E. A. Henchal, V. W. Weedn, M. A. Northrup and P. Belgrader, Anal. Chem., 1998, 70, 2013–2017.
- W. Liu and D. A. Saint, Biochem. Biophys. Res. Commun., 2002, **294**, 347–353.
- 47 J. Wilhelm, A. Pingoud and M. Hahn, BioTechniques, 2003, 34, 324-332.